Supporting Information for

Photoactive Monofunctional Pt(II)-Cyanine Complex for Nucleus and Mitochondria Dual-Targeted Antitumor Therapy

Ting He‡, Qiaoju Ren‡, Yu Zhang‡, Qinan Tang, Chao Jiang, Yurong Liu, Ziguang Wang, Shan Lei, Yifan Zhang, Peng Huang, and Jing Lin*

Marshall Laboratory of Biomedical Engineering, International Cancer Center, Laboratory of Evolutionary Theranostics (LET), School of Biomedical Engineering, Shenzhen University Medical School, Shenzhen University, Shenzhen, 518055, China.

Materials

2, 3, 3-Trimethyl-2, 3-dihydro-1H-indole, benzyl bromide, phosphorus oxychloride, cyclohexanone, dimethyl pyridine amine, N-(2-bromomethyl) phthalates formyl imide, dipotassium tetrachloroplatinate (K_2PtCl_4), potassium carbonate, sodium sulfate (Na_2SO_4), sodium carbonate, pyridine, N, N-dimethyl formamide, hydrazine, were purchased from Energy Chemical Co. LTD. Concentrated hydrochloric acid, toluene, dichloromethane (DCM), and diethyl ether were purchased from Bolaien Shenzhen Co. LTD. DSPE-PEG2000 was purchased from Ponsure Biotechnology. All aqueous solutions used were prepared from deionized water.

Characterization

^{1}H NMR, ^{13}C NMR, and ^{195}Pt NMR spectra were determined by Bruker AVANCE III superconducting nuclear magnetic resonance spectrometer. HR-MS was determined by MALDI-TOF/TOF 5800 mass spectrometer with a triple quadrupole tandem mass spectrometry system. The morphology of nanoparticles was characterized by biological transmission electron microscope HITACHI-HT7700. The particle size and Zeta potential were characterized by Malvern laser particle size analyser Zeta Sizer Nano ZS90. The UV-vis-NIR absorption spectrum was measured by Agilent Cary 60. The fluorescence spectrum was obtained with Thermo Fisher Scientific F7000 fluorescence spectrophotometer, and both excitation and emission slits were 5 nm. Confocal imaging of cells was achieved using ultra-high resolution confocal laser scanning microscope Zeiss LSM 880. The number of survived cells was measured by BioTek Synergy H1. The cell uptake and ROS staining were characterized by Nikon Eclipse Ti inverted fluorescence microscope. The fluorescence intensity of cells was analysed qualitatively and quantitatively by BD FACS Calibur flow cytometry. The concentration of platinum (Pt) was measured by inductively coupled plasma mass spectrometry (ICP-MS). Fluorescence imaging of various organs and tumor in nude mice was performed by IVIS Spectrum. Real-time photoacoustic (PA) imaging in nude mouse tumor was recorded by using Vevo LAZR X system.

Synthesis of Pt-CDPEN. CDPEN was synthesized according our previous report[46]. The K_2PtCl_4 solution (0.20 g, 0.48 mmol, 5 mL) and CDPEN (0.23 g, 0.24 mmol in

methanol, 10 mL) were stirred for 48 h in dark at room temperature. The mixture was extracted with dichloromethane (DCM), dried with anhydrous Na_2SO_4, and then the solvent was removed by vacuum. The residue was purified by silica gel column chromatography to obtain Pt-CDPEN as a deep blue-green solid (0.17 g, yield 61.0%). ^{1}H NMR (500 MHz, DMSO-d6) δ 8.69 (d, 2H), 8.18 (t, 2H), 8.13 (d, 2H), 7.98 (dd, 4H), 7.78 (d, 2H), 7.67 – 7.63 (m, 2H), 7.59 (d, 2H), 7.55 – 7.51 (m, 2H), 7.47 – 7.38 (m, 7H), 7.31 (dd, 7H), 5.73 (d, 2H), 5.41 (d, 6H), 4.92 (d, 2H), 3.74 (m, 2H), 3.48 (m, 2H), 2.24 (s, 4H), 1.77 (s, 12H), 1.65 – 1.61 (t, 2H). ^{13}C NMR (126 MHz, DMSO-d6) δ 169.52, 168.44, 165.76, 149.64, 141.88, 141.31, 137.77, 136.36, 131.46, 131.07, 130.54, 130.39, 129.40, 128.41, 128.06, 127.99, 127.04, 126.04, 124.30, 124.09, 122.19, 121.16, 111.44, 96.09, 74.86, 68.98, 64.23, 55.41, 49.68, 46.54, 28.27, 25.40, 21.24. ^{195}Pt NMR (108 MHz, DMSO-d6) δ -2321.53. HRMS (ESI) *m/z* = 1171.45178 (calculated for $C_{66}H_{65}N_6ClPt^+$: *m/z* 1171.46015).

Synthesis of LET-9. DSPE-PEG_{2000} solutions (1, 2, 3, or 4 mg/mL) were prepared, respectively. For each ratio, 1 mL of Pt-CDPEN (1 mg/mL in DCM) was added dropwise into 2 mL of DSPE-PEG_{2000} solution at ultrasound condition for 3 min. Then DCM was removed under nitrogen bubble, and filtered through a polyethersulfone filter membrane (0.22 μm), then centrifuged and washed for 3 times in a 30 kDa ultrafiltration tube at 4°C for 15 min. The concentration of LET-9 solution was determined by UV-vis-NIR spectrophotometer. The sample was stored at 4°C away from light.

Theoretical calculations. The optimization was conduct by DFT calculations using B3LYP/LanL2DZ (for Pt atom) and 6-31G (for other atom) with Gaussian G16 system.

$^1O_2$ detection and quantitative analysis. $^1O_2$ quantum yield was detected by 1,3-diphenylisobenzofuran (DPBF) probe. DPBF (60 μM in acetonitrile) was mixed with same optical density (OD) at 635 nm of CDPEN (1.6 μM), Pt-CDPEN (1.0 μM) or MB (0.5 μM). The mixture was measured under 635 nm laser irradiation (0.2 W cm^{-2}). The

absorption curves of DPBF with different irradiation time were measured and calculated by equation 1.

$$\phi_{\triangle}(^1O_2)^{LET\text{-}9}=\phi_{\triangle}(^1O_2)^{MB}\bullet(S^{LET\text{-}9}F^{MB})/(S^{MB}F^{LET\text{-}9}) \quad (1)$$

$\phi_{\triangle}(^1O_2)$ is the singlet oxygen yield, superscript "MB" represent methylene blue, "S" is the slope of the absorbance of DPBF at 413 nm with time, "F" is the absorbance correction factor, is obtained from $F = 1\text{-}10^{-OD}$ (OD is the absorbance of the sample or reference sample at 635 nm). The $^1O_2$ quantum yield of reference probe MB in acetonitrile solution is 0.52. According to the equation 1, the quantum yield of Pt-CDPEN is 0.21.

$^1O_2$ detection by ESR. Pt-CDPEN (1 μM in acetonitrile) or LET-9 solution was mixed with 10 mM of 2, 2, 6, 6-tetramethylpiperidine (TEMP) acetonitrile solution. Then the mixture was irradiated by 635 nm laser (0.2 W cm^{-2}) for 1 min before ESR analysis.

***In vitro* assays of cytotoxicity and therapy.** 4T1, A549 and A459DDP cells were cultured in DMEM containing 10% (*v*/*v*) FBS and penicillin-streptomycin (100 μg/mL) at 37°C in 5% CO_2 atmosphere. 5×10^3 cells per well were seeded in 96-well plates and incubated overnight. After washed with PBS (pH 7.4), the cells were incubated with various concentrations of Cis-Pt, Pt-CDPEN, LET-9 (0, 2.5, 5, 10, 20, and 40 μM). The cell viabilities were measured using MTT assay. For laser group, the cells were exposed to 635 nm laser irradiation (0.2 W cm^{-2}, 5 min) after being incubated with LET-9 for 4 h. The cells were then incubated for further 20 h. The cell viabilities were measured by MTT assay.

Cell uptake and localization of LET-9. For cell uptake, the cells incubated with 20 μM of LET-9 were observed by laser scanning confocal microscope (LSCM) at 0, 2, 4, and 8 h. For lysosomal localization, the cells incubated with 20 μM of LET-9 for 1 h were irradiated with 635 nm laser (0.2 W cm^{-2}) for 5, 10 min, and then stained by Lyso-Tracker Red probe for lysosomes before observed by LSCM. The dark groups were incubated for 1 h or 24 h before LSCM observation. The lysosomal colocalization ratio

was analysed by ImageJ software. For mitochondrial localization, the same condition excepted the stained dye replaced with MitoTracker Red probe for mitochondria.

Intracellular ROS production and DNA damage. For ROS detection, the 4T1 cells incubated with PBS or LET-9 (20 μM) for 4 h were irradiated by 635 nm laser for 5 min, then stained with 2',7'-dichlorofluorescin diacetate (DCFH-DA) dye for 30 min and fixed with 4% formaldehyde before observation of LSCM. For DNA damage, the 4T1 or A549DDP cells incubated with PBS, Cis-Pt, Pt-CDPEN, LET-9 (10 μM) after 4 h were irradiated by 635 nm laser for 5 min, then incubated with another 4 h before Triton X-100 PBS permeabilized and blocked with 1% BSA PBS solution for 2 h. The samples were stained by γH2AX antibody for incubation overnight, and then the secondary antibodies were labelled by Alex Four 488. All FL images were recorded by high content instrument.

Measurement of DNA platination by ICP-MS. The A549DDP cells were treated by 20 μM of Cis-Pt, Pt-CDPEN, or LET-9 for 4 h and then treated with or without laser irradiation (635 nm, 10 min, 0.2 W cm^{-2}). After another 4 h incubation, all cells (including dead cells) were collected and counted. The DNA of collected cells was extracted by Genomic DNA Mini Preparation Kit. The Pt concentration in DNA was measured by ICP-MS.

***In vivo* imaging.** All animal experiments were approved by the Animal Ethical and Welfare Committee of Shenzhen University (AEWC-SZU) and complied with all relevant policies and regulations. 4T1 tumor-bearing nude mice were intravenously injected with Pt-CDPEN or LET-9 (10 mg/kg). 1% Tuwen-80 was added in Pt-CDPEN to improve its solubility. FL images were collected at 0, 2, 8, 12, 24, and 36 h using a small animal FLI system (IVIS Spectrum, λ_{ex} = 690 nm, λ_{em} = 800 nm) and PA images were collected at 0, 1, 2, 4, 8, 12, 24, and 36 h using PAI system (VisualSonics Vevo LAZR X, PA signal at 715 nm). PA signals of different concentrations of LET-9 (0.02~1.6 mg/mL) were also obtained using the small animal PAI system.

***In vivo* treatment.** The therapeutic effects of LET-9 were examined in 4T1 tumor bearing mice. A total of 25 mice were randomly divided into 5 groups (PBS, Cis-Pt, Pt-CDPEN, LET-9, and LET-9+laser) with 5 mice per group. LET-9 was administered at a dose of 10 mg/kg. The laser group received 635 nm laser irradiation at a density of 0.2 W cm^{-2} for 20 min. The body weights and tumor volumes of the mice were measured every two days to evaluate the therapeutic performance. After treatment, all mice were euthanized, then the tumor and major organs were removed for histological and statistical analysis.

Evaluation of biotoxicity. Five healthy mice were intravenously administered LET-9 (10 mg/kg) via tail vein, and blood was collected (approximately 200 μL) at day 0 and 14 post-injection (p.i.). The blood was tested with following parameters: alanine aminotransferase (ALT), aspartate aminotransferase (AST), blood urea nitrogen (BUN), and creatinine (CRT).

Statistical analysis. The quantitative data were expressed as mean ± standard deviation. Student's t-test (cell data) and two-way ANOVA (animal data) analysis were applied through GraphPad Prism 6.0 to determine the significant difference between different experimental groups. p-value less than 0.05 was considered statistically significant ($p^* < 0.05$, $p^{**} < 0.01$, $p^{***} < 0.001$, and $p^{****} < 0.0001$).

Supplementary Figures

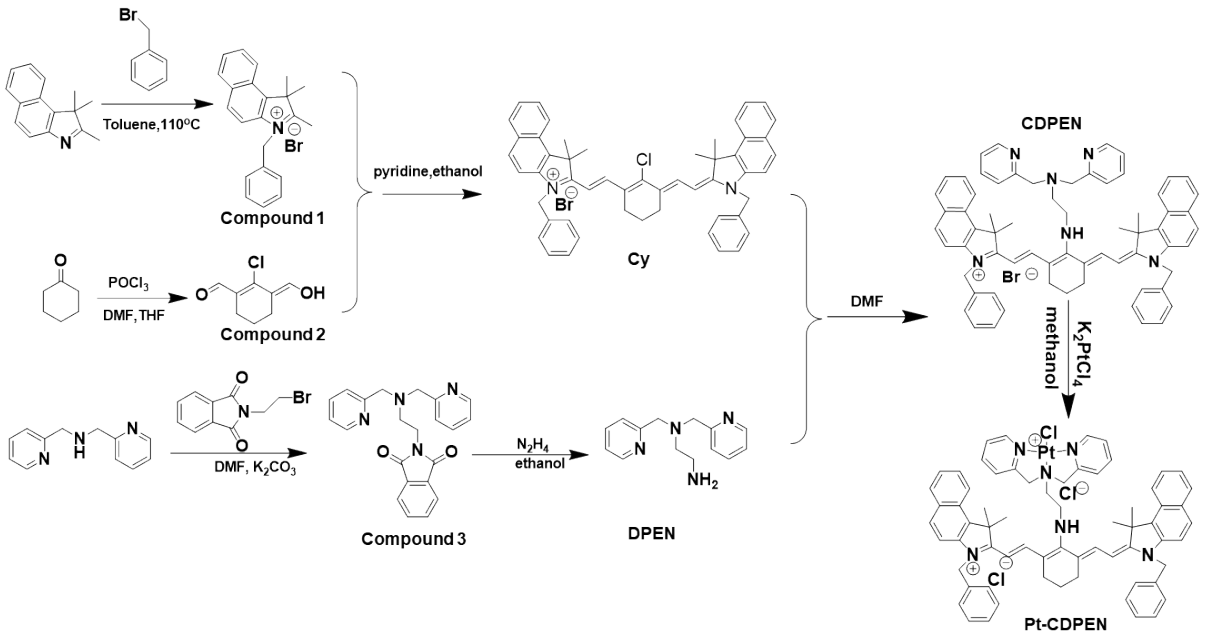

Fig. S1 The synthesis route of Pt-CDPEN.

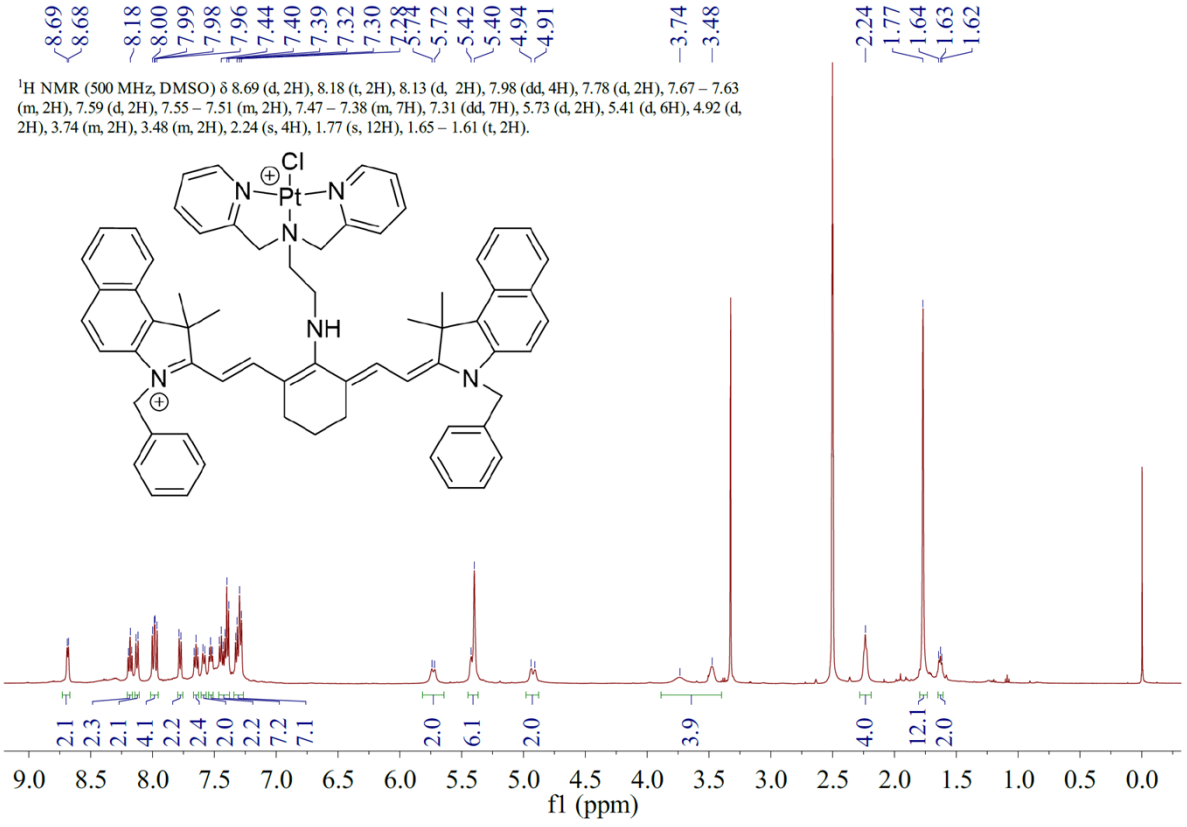

Fig. S2 ^{1}H NMR spectrum of Pt-CDPEN in DMSO-d6.

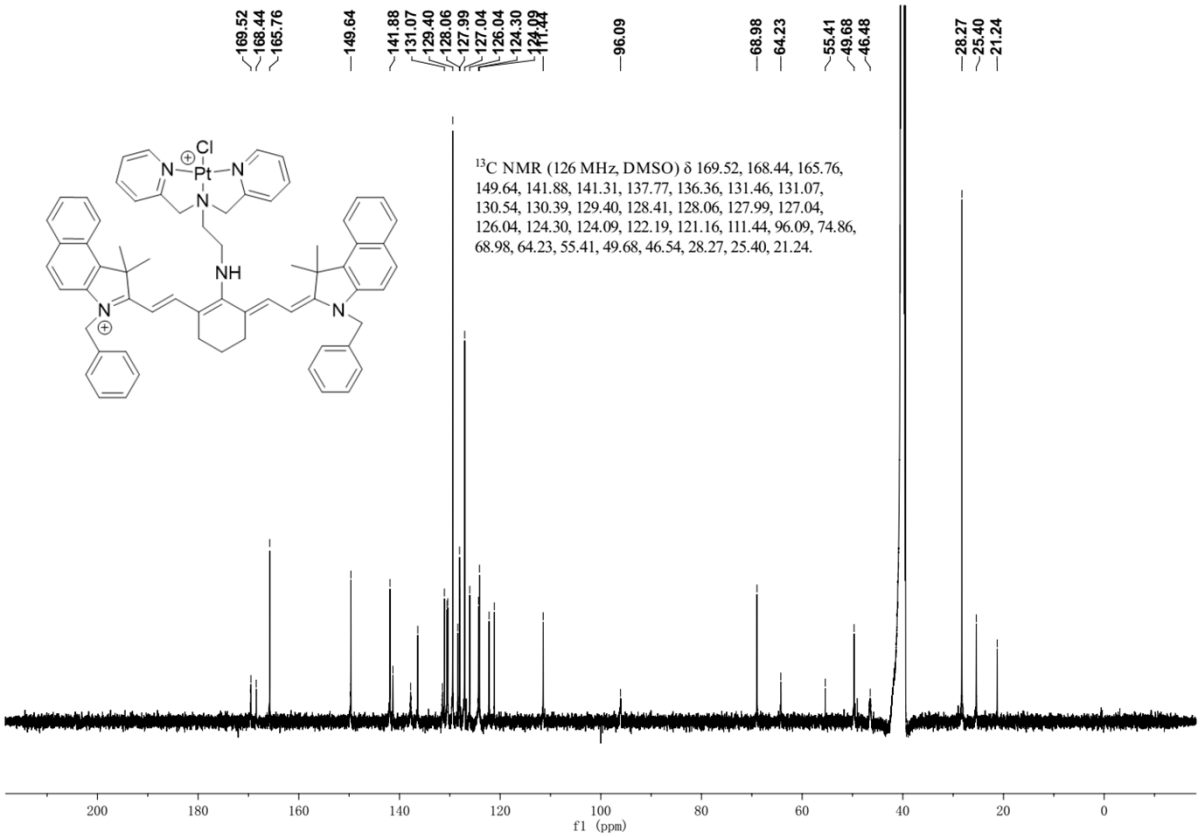

Fig. S3 ^{13}C NMR spectrum of Pt-CDPEN in DMSO-d6.

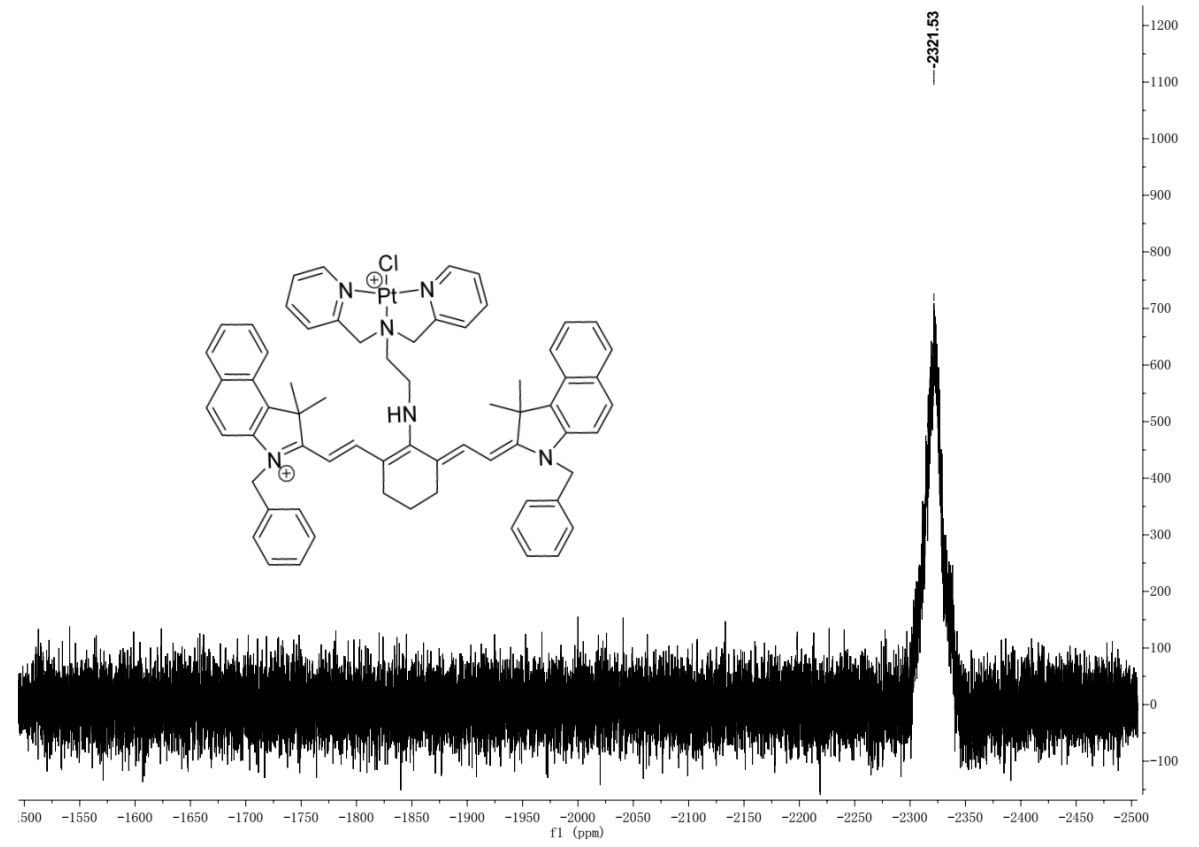

Fig. S4 ^{195}Pt NMR spectrum of Pt-CDPEN in DMSO-d6.

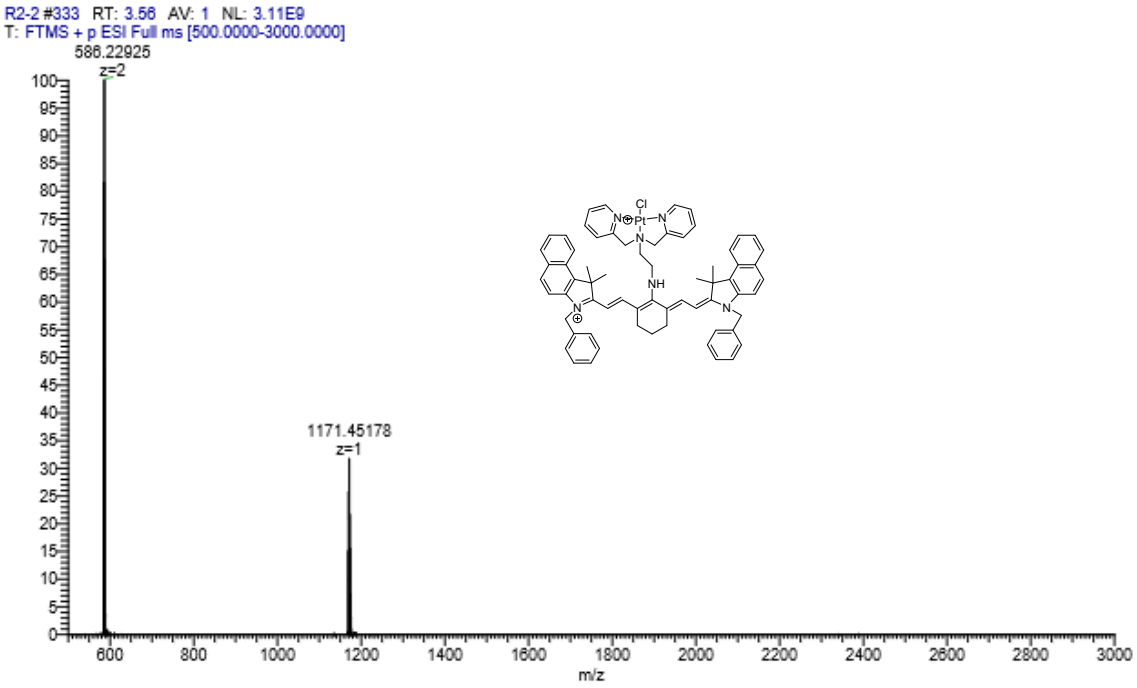

Fig. S5 HR-MS spectrum of Pt-CDPEN.

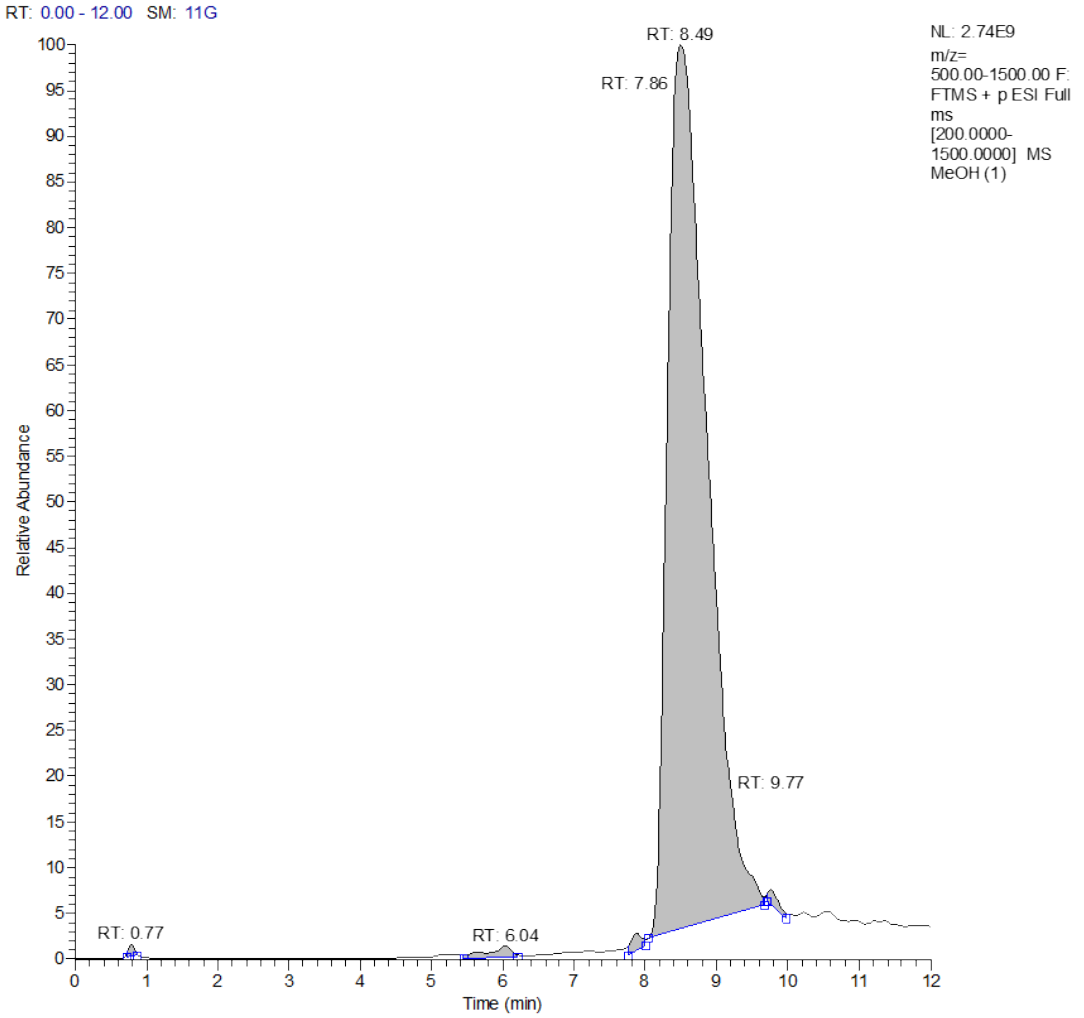

Apex RT	Start RT	End RT	Area	%Area
0.77	0.73	0.86	196575400.411	0.19
6.04	5.45	6.20	871434488.017	0.83
7.86	7.76	8.00	546570095.361	0.52
8.49	8.04	9.67	102405211931.372	97.99
9.77	9.71	9.97	489613581.004	0.47

Fig. S6. The HPLC result of Pt-CDPEN.

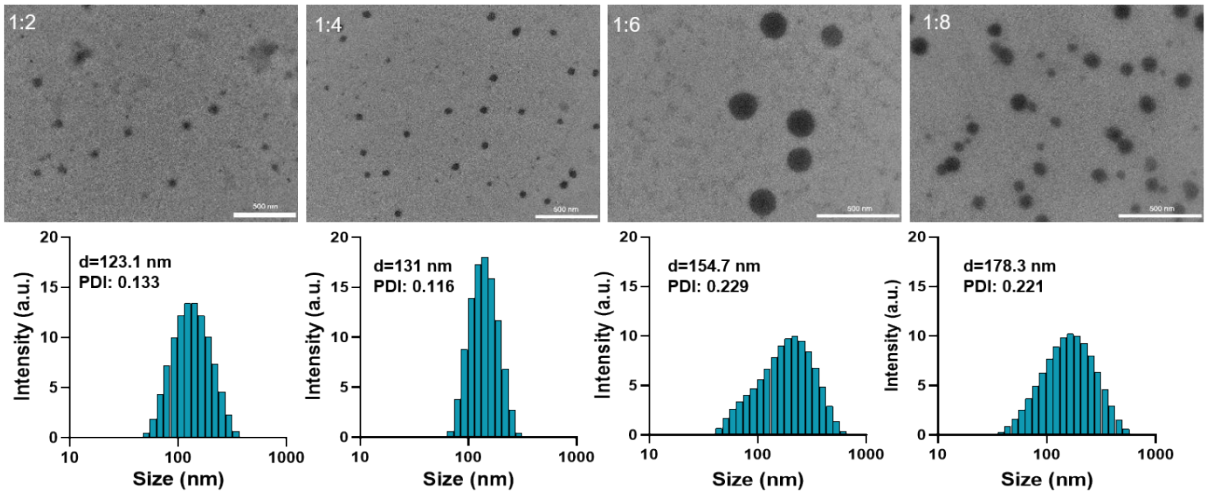

Fig. S7 TEM images of assembled nanoparticles with various ratios of Pt-CDPEN and DSPE-PEG$_{2000}$ and their hydraulic diameters.

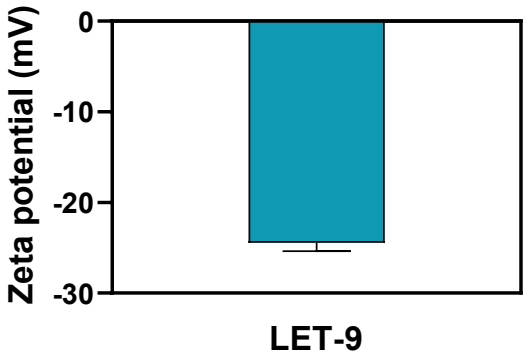

Fig. S8 The zeta potential of LET-9.

Compounds	HOMO	LUMO
CDPEN	-5.213 eV	-2.629 eV
Pt-CDPEN	-4.226 eV	-2.156 eV

Fig. S9 The calculated HOMO and LUMO energy of CDPEN and Pt-CDPEN, respectively.

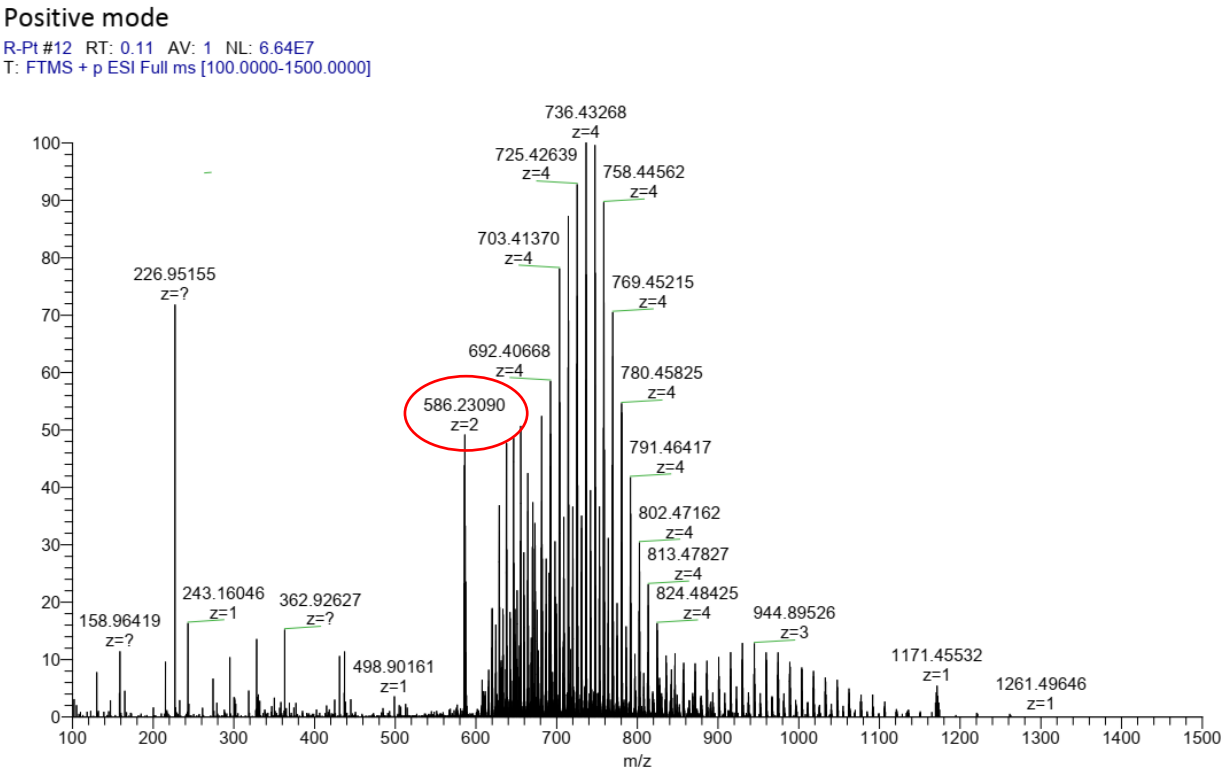

Fig. S10 HRMS of LET-9 before irradiation.

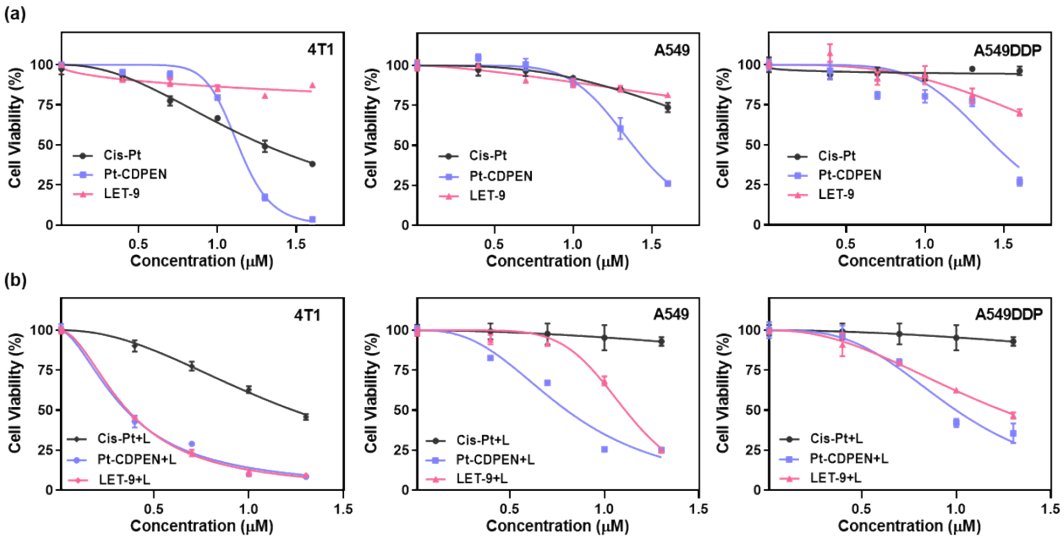

Fig. S11 (a) Cell viabilities of 4T1, A549 and A549DDP cells incubated with Cis-Pt, Pt-CDPEN, and LET-9, respectively. (b) Cell viabilities of 4T1, A549 and A549DDP incubated with Cis-Pt, Pt-CDPEN, and LET-9, respectively, with laser irradiation (635 nm, 0.2 W cm^{-2}, 10 min).

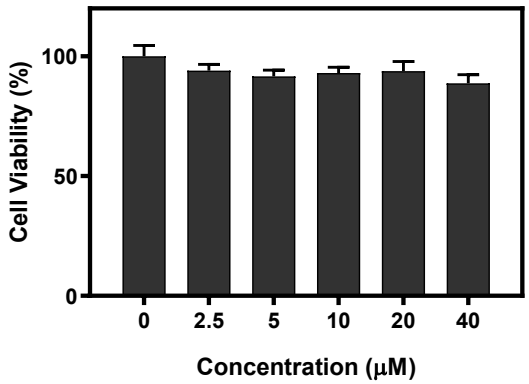

Fig. S12 Cell viability of HEK293T cells incubated with different concentration of LET-9.

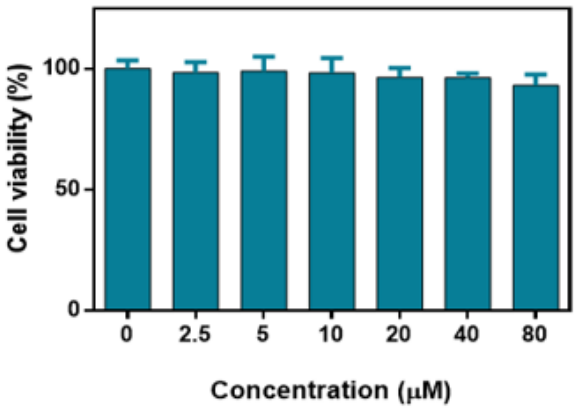

Fig. S13 Cell viability of A549DDP cells incubated with different concentration of Cis-Pt in dark.

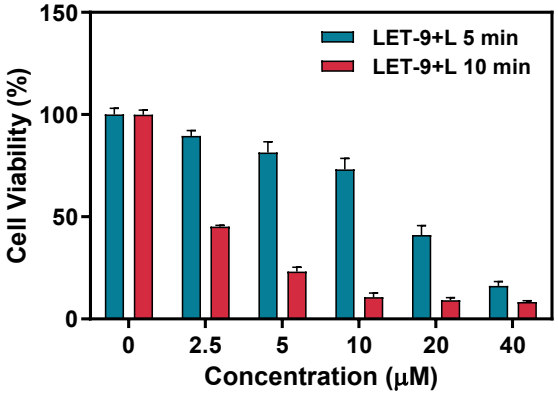

Fig. S14 Cell viabilities of 4T1 cells incubated with LET-9 for 4 h then irradiated with 635 nm laser for 5 or 10 min.

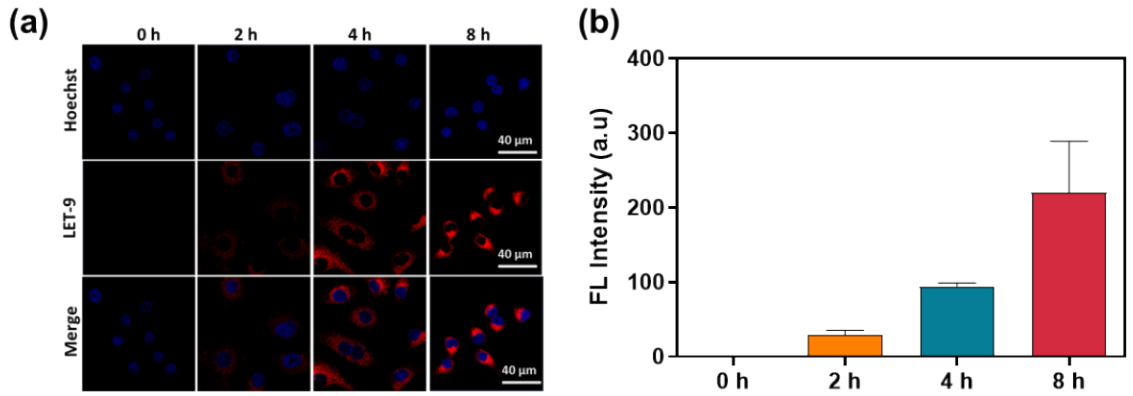

Fig. S15 (a) The fluorescence images of 4T1 cells incubated with LET-9 detected by LSCM and (b) its quantitative analysis.

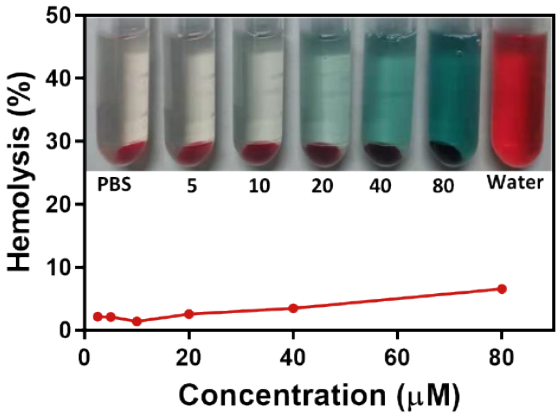

Fig. S16 The hemolysis assay of LET-9 at different concentrations.

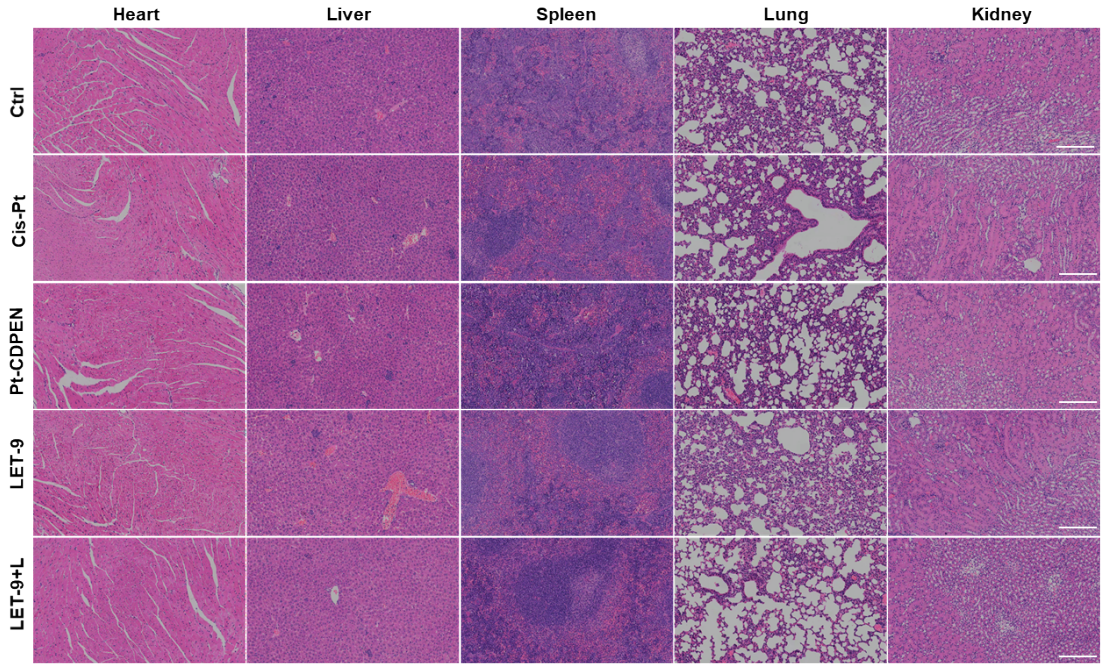

Fig. S17 The H&E stained sections of main organs (heart, liver, spleen, lung, and kidney) after treatments. Scale bar: 200 μm.